Modeling and Characterization of an Electrooptic Polarization Controller on $LiNbO_3$

Arjan J. P. van Haasteren, Jos J. G. M. van der Tol, M. Oskar van Deventer, and Hans J. Frankena

Abstract—**A model for describing the operation of an integrated electrooptical polarization controller on $LiNbO_3$ as a function of the applied voltages is presented. This model contains several parameters; for their determination, a special measurement procedure has been developed. This technique is used to determine the parameters of a developed polarization controller. With these parameters, the model describes the operation of the controller accurately. Moreover, the model can be used to calculate the voltages needed to reach a specific polarization conversion.**

I. Introduction

OPTICAL coherent detection communication systems attract much attention because of their increased receiver sensitivity and wavelength selectivity as compared with direct detection communication systems [1], [2].

A complication of the coherent technique is the required polarization match between the transported optical signal and that coming from the local oscillator. Since the state of polarization (henceforth referred to as SOP) of the transported signal fluctuates as a result of changes in the temperature, stress and humidity of the fiber, a fading of the output electrical signal occurs. Several techniques to overcome this problem are known: polarization diversity, data-induced polarization switching, polarization scrambling, use of polarization maintaining fibers and use of a polarization controller [3]–[7]. From these techniques the one using a polarization controller yields the best receiver sensitivity. Until now mechanical polarization controllers have been realized, using electrical fiber squeezers, fiber cranks which can be rotated or polarization preserving fibers wound around piezo-electrical cylinders [7]–[9]. To keep receivers small, reliable and operating at low voltages (< 100 V), however, an integrated broad-band optical polarization controller on a lithium niobate ($LiNbO_3$) substrate [10], [11] is the most likely candidate for future production. Moreover, such controllers can also be used in (multilevel) polarization shift keying [12], [13].

A typical integrated, broad-band polarization controller on $LiNbO_3$ is shown in Fig. 1. It consists of an X-cut substrate with a titanium diffused channel waveguide in the Z-direction. Two electrodes have been placed along and one directly above the waveguide. If voltage differences are applied between these electrodes, an electric field is generated in the $LiNbO_3$ which alters its index ellipsoid. Because of this electrooptic effect

Manuscript received May 19, 1992; revised December 28, 1992.

A. J. P. van Haasteren and H. J. Frankena are with Delft University of Technology, Department of Applied Physics, 2600 GA Delft, The Netherlands.

J. J. G. M. van der Tol and M. O. van Deventer are with PTT Research, Leidschendam, The Netherlands.

IEEE Log Number 9209882.

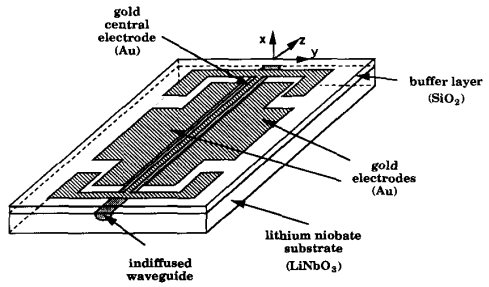

Fig. 1. An integrated optical polarization controller on X-cut, Z-propagating $LiNbO_3$

[14], a wave coupled into the waveguide generates two linearly and mutually perpendicular, polarized waves which propagate with different phase velocities. The magnitude and the direction of the external electric field determine the polarization direction of these waves and their phase difference at the end of the waveguide. Hence, the SOP of the light emanating from the waveguide depends on and can be controlled by the voltage differences between the electrodes.

For the application [15] of polarization controllers in coherent detection communication systems or in polarization shift keying systems, a thorough analysis of the controller's operation is necessary. Here, we develop a model describing systematically the polarization conversion as a function of the voltage differences. Using this model the voltage differences required for realizing a certain polarization conversion can be calculated so that the use of a trial and error algorithm [16] can be avoided.

In the derived model, the influence of the electrooptic effect and of the characteristics of the waveguide, i.e., dichroism and birefringence, on the polarization conversion is described in terms of several parameters. For the determination of these, a new measurement procedure has been developed. For a specifically developed polarization controller, the parameters have been determined with which the model describes the actual polarization conversion accurately.

II. The Model

The voltage differences between the electrodes cause a deformation of the index ellipsoid [14]. Consequently, two linearly, mutually orthogonal, polarized waves propagate through the channel waveguide. Starting from the deformation of the index ellipsoid, the direction along which these two waves are polarized and the corresponding refractive indexes can be

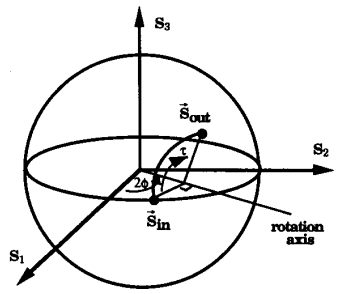

Fig. 2. The polarization conversion as represented on the Poincaré sphere.

calculated. If the directions of the x-, y- and z-axis are chosen along the direction of X-, Y-, and Z-axis (the principal axes of the $LiNbO_3$ crystal), respectively, the waves are polarized in a direction in the xy-plane making angles with the x-axis of ϕ and $\phi+\pi/2$, respectively, where [17] (see the appendix):

$$\phi = \frac{1}{2}\arctan\left(-\frac{\tau_1}{\tau_2+\tau_i}\right). \tag{1}$$

Here, τ_i represents a constant phase retardation between the quasi TE- and TM-polarized waves resulting from the waveguide properties. The retardations τ_1 and τ_2 are given by:

$$\tau_1 = (\omega/c)Lr_{22}n_o^3E_{ex} \tag{2}$$

$$\tau_2 = (\omega/c)Lr_{22}n_o^3E_{ey}. \tag{3}$$

In these formulas, r_{22} is the electrooptical constant [14], n_o is the ordinary refractive index of $LiNbO_3$ ($= 2.2125$ for $\lambda =$ 1523 nm), E_{ex} and E_{ey} represent the x- and y-components of the external electrical field strength, respectively, caused by the voltage differences between the electrodes while ω and c are the frequency and velocity of light in vacuum. Since the two waves propagate with different phase velocities, they show a phase retardation τ at the output of the waveguide which is described by:

$$\tau = (\tau_2+\tau_i)\cos(2_\phi) - \tau_1\sin(2_\phi). \tag{4}$$

Using (1)–(4) the polarization conversion[17] is found to be:

$$\vec{S}_{out} = M\vec{S}_{in} = \begin{bmatrix} \cos^2(2\phi)+\sin^2(2\phi)\cos(\tau) & \frac{1}{2}(\cos(\tau)-1)\sin(4\phi) & \sin(\tau)\sin(2\phi) \\ \frac{1}{2}(\cos(\tau)-1)\sin(4\phi) & \sin^2(2\phi)+\cos^2(2\phi)\cos(\tau) & -\sin(\tau)\sin(2\phi) \\ -\sin(\tau)\sin(2\phi) & \cos(2\phi)\sin(\tau) & \cos(\tau) \end{bmatrix}\vec{S}_{in}, \tag{5}$$

where the normalized Stokes vectors [18] $\vec{S}_{in}$ and $\vec{S}_{out}$ represent the SOP at the controller's in- and output, respectively. On the Poincaré, sphere [18] this polarization conversion is represented by a rotation of $\vec{S}_{in}$ over an angle τ around an axis in the S_1S_2-plane. This axis makes an angle of 2ϕ with the S_1-axis (see Fig. 2).

Although the polarization conversion is well described by (5), a description of the polarization conversion as a function of the voltage differences is of better practical use. Therefore, the parameters τ_1 and τ_2 must be determined as a function of the applied voltage differences. Since the relation between the applied voltage differences and the external electric field

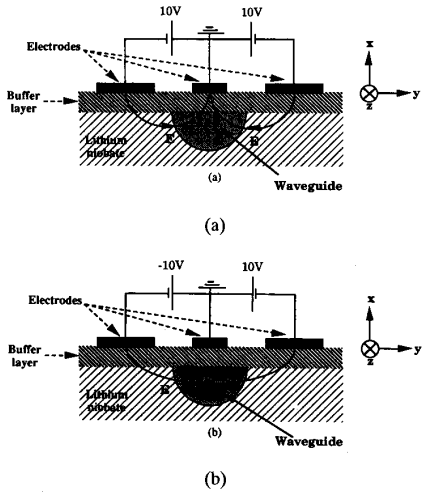

Fig. 3. Schematic of the cross section of the electrodes with (a) a symmetric (U_s=10 V and U_{as}=0 V) and (b) an asymmetric field distribution (U_s=0 V and U_{as}=20 V).

is linear in $LiNbO_3$, this relation can be written with the aid of a tensor T as:

$$\begin{bmatrix}\tau_1\\ \tau_2\end{bmatrix} = T\begin{bmatrix}U_s\\ U_{as}\end{bmatrix} = \begin{bmatrix}t_{11} & t_{12}\\ t_{21} & t_{22}\end{bmatrix}\begin{bmatrix}U_s\\ U_{as}\end{bmatrix}. \tag{6}$$

Here, U_{as} represents the (asymmetrical) voltage difference between the outer electrodes, U_s is the average of the voltages on the outer electrodes with the center electrode grounded and $t_{11}, t_{12}, t_{21}, t_{22}$ represent the elements of the tensor T. The electric field is symmetric along the x-axis when U_{as} is zero and asymmetric if U_s vanishes (see Fig. 3(a) and (b), respectively).

At the waveguide's in- and output sections no electrodes have been placed because of technological limitations. Therefore, the produced polarizer (see Fig. 1), consists of three sections, i.e. two passive sections, at both ends of the waveguide, with an electrooptic section in between. In the passive in- and output sections, two quasi TE- and TM-polarized waves propagate with different phase velocities. Consequently, a phase retardation occurs between those waves which is represented on the Poincaré sphere as a rotation of the SOP around the S_1-axis, where the angle of rotation is determined by the length of the sections and the characteristics of the waveguide. Using normalized Stokes parameters, this rotation can be written as:

$$\vec{S}_{out} = M_{pas}\vec{S}_{in} = \begin{bmatrix}1 & 0 & 0\\ 0 & \cos(\tau_{pas}) & -\sin(\tau_{pas})\\ 0 & \sin(\tau_{pas}) & \cos(\tau_{pas})\end{bmatrix}\vec{S}_{in}. \tag{7}$$

Here, τ_{pas} represents the retardation over a passive section:

$$\tau_{pas} = \nu L_s \tag{8}$$

where:

$$\nu = (n_{TE} - n_{TM})(\omega/c) \tag{9}$$

with L_s representing the length of the passive section while n_{TE} and n_{TM} indicate the effective refractive indexes for TE- and TM-polarized light, respectively. The total polarization conversion obtained with the controller is therefore described by the following relation:

$$\vec{S}_{out} = M_{pas2} M_{act} M_{pas1} \vec{S}_{in}, \tag{10}$$

where M_{pas1}, M_{act}, and M_{pas2} are matrices describing the polarization conversion caused by the first passive section, the active section and the second passive section, respectively (see (5) and (7)).

It should be noted that the polarization convertor is designed for use in coherent systems. Consequently, the intensity of the emanating light may not depend on the SOP, so the convertor is assumed not to show a perceptible dichroic effect [18].

III. Design and Fabrication of the Polarization Controller

A. Waveguide Design

While concentrating on the usual communication wavelength of 1523 nm, the polarization controller's design received much attention to avoid dichroism. Moreover, the mode diameter was kept small to assure a strong electrooptic interaction. There is, however, a lower boundary to that diameter determined by the maximum allowed coupling loss between waveguide and fiber (i.e., 1.0 dB).

The characteristics of the waveguide, which is fabricated by local diffusion from a strip of titanium (Ti) placed on top of the $LiNbO_3$-substrate, depend on the height and width of that Ti-strip and on the diffusion conditions (temperature and time). The optimal values for these parameters have been determined with the following procedure. From the diffusion parameters a refractive index profile is calculated [19] from which the dimensions of the mode field are determined with the effective index method.

For a Ti-strip with a width of 9 μm and a height of 70 nm and a diffusion time and temperature of 1000°C and 16 hours, respectively, a mono-mode waveguide is fabricated which does not show a dichroic effect. The fiber to chip coupling loss has been measured and it turned out to be smaller than 1 dB.

B. Buffer Layer Design

If the electrodes are placed directly on top of the waveguide, a strong interaction occurs between the metal and the propagating waves. Since such an interaction causes a loss difference between TE- and TM-polarized light (dichroism), it has to be prevented. To overcome this problem, a buffer layer in which the optical field decreases rapidly is evaporated on the substrate before the metal layers are deposited.

The buffer layer material must have a low refractive index to assure a fast decrease of the optical field. On the other hand, the permitivity should be large to assure that the voltage differences between the electrodes cause a large external electric field. As a compromise, quartz (SiO_2) has been chosen ($n = 1.46, \varepsilon = 4.00$).

To maintain a strong electricoptic effect, a thin buffer layer must be used. There is, however, a lower limit above which the attenuation of TE- and TM-polarized light is approximately equal. The attenuation of a TE- and a TM-wave was calculated for a model of the channel waveguide, i.e., a planar waveguide, covered by a buffer layer of SiO_2 upon which a metal layer of 1 nm titanium and 100 nm gold was deposited. This calculation has been performed using complex calculus and a transfer matrix approach for several thicknesses of the buffer layer. From the results, a value of 100 nm was found for the lower limit of the buffer layer thickness.

After fabrication of the polarization controller, the difference in attuation of TE- and TM-polarized light has been experimentally determined and was found to be negligible.

C. Electrode Design

On top of the buffer layer three gold electrodes are deposited (first a thin layer of titanium (1 nm) is evaporated to assure a good attachment of the electrodes): two symmetrically along the waveguide and one on top of it. This electrode structure is optimized for electrooptical interaction via a finite difference solution of the Laplace equation and the overlap integral. The optimal width of the central electrode turned out to be 6 μm and the optimal distance between the middle electrode and the side electrodes was found to be 4 μm. One parameter remained to be determined, i.e. the length of the electrodes. For realizing polarization control a retardation range of 2π is required[12]. The attainable values of the external electric field are limited by the range of voltages that can be safely applied to the device. The length of the electrodes must therefore be chosen such that a retardation of at least 2π is obtained if the electric field is maximal. On the basis of experience and simulations, the range of voltage differences between two adjacent electrodes that can be applied was found to be -35 to 35 V. Using these results and electrooptic simulations mentioned above, a minimum electrode length of 1.25 cm was found. To be on the safe side, an electrode length of 2.0 cm has been chosen.

IV. Measurement Configuration

The model contains six parameters, i.e. $t_{11}, t_{12}, t_{21}, t_{22}, \tau_i$ and ν (see (1), (6), and (9)). Since these parameters depend on the characteristics of $LiNbO_3$, the waveguide and the position of the electrodes, they have to be determined experimentally. For this, a special measurement procedure has been developed.

For coupling of light into the waveguide of the controller, a polarization maintaining fiber is used (see Fig. 4). By positioning the fiber TE- or TM-polarized light, necessary for the determination of the parameters, can be coupled into the waveguide.

The SOP of the light emanating from the controller is described by its Stokes parameters. These parameters are measured with a polarizer and a quarter-wave plate.

First, the polarizer is rotated to measure the extinction ratio R and the angle of maximum extinction α, yielding S_1, S_2 and the absolute value of S_3:

$$S_1 = \frac{R-1}{R+1}\cos(2\alpha), \tag{11}$$

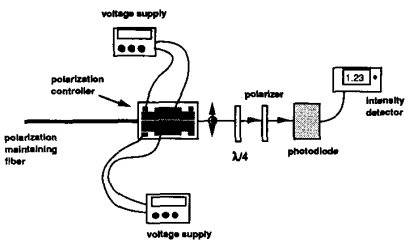

Fig. 4. The measurement configuration for determining the parameters of the model.

$$S_2 = \frac{R-1}{R+1}\sin(2\alpha), \tag{12}$$

$$S_3 = \pm\sqrt{1 - S_1^2 - S_2^2}. \tag{13}$$

Then, the quarter-wave plate is inserted to determine the sign of S_3.

V. Measurement Procedure and Results

The two voltages applied to the device can not be translated unambiguously to the fields in the waveguide, because of possible misalignment errors of the electrodes (see (6)). Therefore, the SOP is expected to describe rather complicated and untractable trajectories on the Poincaré sphere as a function of applied voltages. To determine the behaviour of the device in terms of the model parameters it appeared necessary to develop the following special measurement procedure.

For determination of the parameters, use has been made of the fact that without applied voltages the only effect of the device is a phase shift between the quasi TE- and the TM-polarized waves. This is a consequence of the symmetry of the waveguide. It is therefore possible to couple one of these polarizations into the waveguide and observe the same polarization in the output SOP with both voltages being zero.

The determination of the parameters now proceeds along the following steps:

- 1° Within the specified range $[-35V, 35V]$ that can be safely applied without the danger of breakdown, the voltages are adjusted such that the output SOP is equal to the input SOP. Since the input SOP is either TE or TM, for these combinations of voltages no TE-TM coupling takes place, but only a change in the phase. In this way, the line in the U_s, U_{as}-diagram with zero TE-TM coupling (see Fig. 5) is determined. Along this line the following equation holds, see (6):

$$t_{11}U_s + t_{12}U_{as} = 0. \tag{14}$$

  Note that in this step the two passive sections have no influence because only TE- or TM-polarized light propagates through these sections.

  From the experimental determination of this line the ratio of the two matrix elements t_{11} and t_{12} is determined as:

$$\frac{t_{11}}{t_{12}} = 9.8.$$

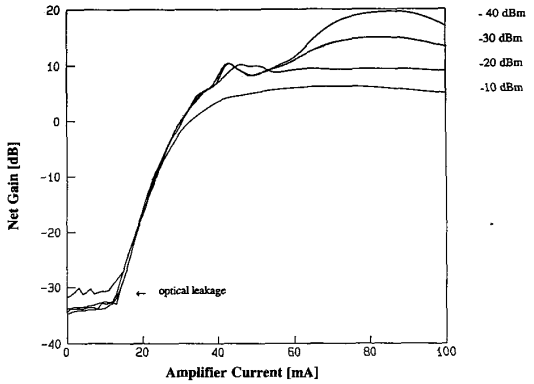

Fig. 5. Measurement results (the solid lines represent least squares fits).

- 2° As a second step, with the same input SOP, the voltages are both changed along a line in the U_s, U_{as}-diagram which is parallel to the 'zero coupling'-line determined in the previous step. Since the device is linear this means that a fixed amount of TE-TM coupling occurs, i.e., τ_1 has a fixed value, while the phase shift $(\tau_2 + \tau_i)$, where τ_i represents the intrinsic birefringence of the diffused channel waveguide, see (1), changes as a function of the applied voltage differences. Along this line the point is determined which gives the maximum TE-TM conversion, i.e., the point were the output SOP is closest to the polarization orthogonal to the input SOP. This point can easily be determined by measuring the maximum intensity on the detector with the output polarizer in the orthogonal position with respect to the input SOP. A phase shift in the electrooptic section deteriorates the TE-TM conversion. Therefore, the maximum TE-TM conversion indicates a combination of voltages where the phase shift vanishes, i.e., $\tau_2 + \tau_i = 0$. By repeating this procedure with a number of lines for fixed TE-TM coupling, a second line (see Fig. 5) can be determined in the U_s, U_{as}-diagram which gives zero phase shift, see (6):

$$t_{21}U_s + t_{22}U_{as} + \tau_i = 0. \tag{15}$$

  The passive section at the input still has no influence on this line, since only TE- or TM-modes pass this section. Also the passive section at the output has no influence, since one has only to determine the intensity in the TE- and TM-modes, without needing to know their relative phases.

  From the experimental results the following ratios have been found:

$$\frac{t_{21}}{\tau_i} = -0.0039V^{-1},$$

$$\frac{t_{22}}{\tau_i} = 0.021V^{-1}.$$

- 3° Then, with the same input SOP the output SOP is determined along the line in the U_s, U_{as}-diagram for which the phase shift is zero (i.e., the line determined in the second step where $\tau_2 + \tau_i = 0$). In that case the device

performs two actions in series. First, a TE-TM coupling takes place which is induced electrooptically and whose strength is proportional to the distance in the U_s, U_{as}-diagram from the line determined in Step 1, the line with zero TE-TM coupling. Second, a phase retardation occurs resulting from the passive section at the output. Since the TE-TM coupling is entirely determined by the active section the proportionality constant for this coupling can be determined from the measured retardation τ_1, which is the rotation around the S_2-axis of the Poincaré sphere. From this, the values of t_{11} and t_{12} are determined using the ratio found in Step 1:

$$t_{11} = 0.167 \text{ rad } V^{-1},$$
$$t_{12} = 0.017 \text{ rad } V^{-1}.$$

If TE-TM coupling was the only action of the device, the output SOP would contain no S_2-component. However, the phase retardation in passive section at the output gives a rotation $\tau_{pas,2}$ around the S_1-axis, which results in a S_2-component. With this component the retardation resulting from this passive section is determined. Again there is no influence of the passive section at the input. It is found that the extra retardation due to the final passive section is $(-0.18 \pm \text{m}2\pi)$ rad, where m is an integer. Comparison with simulations and with the value of τ_i, which follows in the next step, show that m = 0 in this case.
Knowing the length of the final passive section the value of the constant ν from (8) is found:

$$\nu = -0.36 \text{ rad mm}^{-1}$$

- 4° Only one parameter remains to be determined. This is the proportionality constant for the electrooptically induced phase shift τ_2. It is determined by changing the input polarization to equally strong TE- and TM-modes. Both these modes are coupled into the waveguide. In this case, the phase shift, which occurs if no voltages are applied, results in an output SOP which has no S_1-component. The voltages are then adjusted along the line of zero TE-TM coupling $\tau_1 = 0$. Comparing the rotation of the SOP around the S_1-axis for small changes of the applied voltages, the required constant can be determined. Using the ratios determined in Step 2 the intrinsic birefringence is found as:

$$\tau_i = -7.21 \text{ rad.}$$

Since the length of the electrooptical section is 20 mm this value is in perfect agreement with the retardation in the passive section, showing that the presence of the electrodes does not influence the intrinsic birefringence of the waveguide.

Summarizing the experimental results in terms of the model, the following behavior is found. First, the guided mode traverses a passive section with a length of 0.9 mm which causes a phase shift of -0.32 rad. Then, the electrooptic section is entered where simultaneously two retardations occur, i.e., τ_1 and $(\tau_2 + t_i)$, a TE-TM coupling and a TE-TM phase retardation, respectively, which are given by:

$$\tau_1 = 0.167U_s + 0.017U_{as} \quad \text{[rad]},$$
$$\tau_2 = 0.028U_s - 0.151U_{as} - 7.21 \quad \text{[rad]},$$

with the $U's$ expressed in volts. Finally in the last passive section with a length of 0.5 mm, an extra phase shift occurs of -0.18 rad.

With the parameters given above the model can be used to predict the operation of the device as a function of the incoming SOP and the applied voltages. Inversely, the voltages needed to reach a specific polarization conversion can easily be obtained. As an example, we used the model to calculate the voltages for 100% TE-TM conversion. Within the allowed voltage ranges two such states are predicted. At $U_s = -13.7$ V and $U_{as} = -50.3$ V, as given by the model, the intensity of the unwanted polarization is less than 0.5% that of the dominating one. At the other predicted state, $U_s = 23.2$ V and $U_{as} = -43.3$ V, the same result is obtained. This means that the predicted output SOP is very close (within 0.1 rad) to the actual SOP.

VI. Conclusions and Discussion

A model has been developed to describe the operation of an integrated electrooptical polarization controller on $LiNbO_3$ as a function of the applied voltages. This model describing a controller consisting of three sections (two passive sections at both ends of the controller with an active section in between) contains six parameters. Four of these describe the electrooptic interaction, one parameter describes the influence of the passive sections on the polarization conversion and one parameter accounts for the intrinsic birefringence caused by the channel waveguide in the active section. For the determination of these parameters a special measurement procedure has been developed which is based upon coupling TE- or TM polarized light into the controller and monitoring the output state of polarization for specific voltage differences between the electrodes. Using this technique, the parameters of a specifically developed polarization controller have been measured. With these parameters, the model predicts the operation of the controller as a function of the incoming SOP and the applied voltages. Moreover, the voltages required for realizing a certain polarization conversion can be calculated. Tests have shown that the actual SOP emanating from the controller is within 0.1 rad of the SOP predicted by the model.

For using the polarization controller in actual applications [15], it has to be packaged. It is important that this is done without causing any strain in the controller, since otherwise the parameters will be altered. It is not required, however, to control the temperature. Firstly, a temperature change of 100°C causes a change in the electrooptical constant [20] r_{22} of only 5%. Moreover, simulations have shown that temperature fluctuations have no influence on the retardation caused by the birefringence of the waveguide. Finally, theory shows that the expansion of the waveguide resulting from an increase in temperature of 100°C gives rise to a change in the retardation of 0.1%, such that this effect can be ignored,

too. Hence, in use at normal room temperatures, the effects of temperature changes on the parameters can be neglected.

APPENDIX

If an external electric field E_e with components in the x- and y-direction is applied inside $LiNbO_3$, the index ellipsoid of this material transforms into [14], [17]:

$$\frac{1}{n_1^2}x^2 + \frac{1}{n_2^2}y^2 + \frac{1}{n_3^2}z^2 + \frac{2}{n_4^2}yz + \frac{2}{n_5^2}xz + \frac{2}{n_6^2}xy = 1 \tag{A1}$$

where

$$\frac{1}{n_1^2} = \frac{1}{n_0^2} - r_{22}E_{ey}, \qquad \frac{1}{n_2^2} = \frac{1}{n_0^2} + r_{22}E_{ey}$$
$$\frac{1}{n_3^2} = \frac{1}{n_e^2}, \qquad \frac{1}{n_4^2} = r_{51}E_{ey}$$
$$\frac{1}{n_5^2} = r_{51}E_{ex}, \qquad \frac{1}{n_6^2} = r_{22}E_{ex} \tag{2}$$

Here, r_{22} and r_{51} represent the electrooptical constants, n_0 and n_e are the ordinary and extraordinary refractive indexes, respectively, while E_{ex} and E_{ey} indicated the x- and y-components of the external electrical field strength. Through the waveguide two mutually perpendicular, linearly polarized waves can progate in the z-direction. The polarization direction and the phase velocities of these waves can be determined from the cross section of the index ellipsoid with the xy-plane which is ellipcal and can be described by:

$$\left(\frac{1}{n_0^2} - r_{22}E_{ey}\right)x^2 + \left(\frac{1}{n_0^2} + r_{22}E_{ey}\right)y^2 - r_{22}E_{ex}xy = 1. \tag{A2}$$

The direction of the principal axes of this ellipse are the polarization directions ϕ and $\phi+\pi/2$ (representing the angles with the x-axis) of the propagating waves, where

$$\phi = \frac{1}{2}\arctan\left(-\frac{\tau_1}{\tau_2}\right). \tag{A3}$$

The state of polarization of the light emanating from the waveguide is determined by ϕ and retardation τ. From (A2) and (A3) follows:

$$\tau = \tau_2 \cos(2\phi) - \tau_1 \sin(2\phi). \tag{A4}$$

Equations (A3) and (A4) only holds for waveguides which do not show a dichroic effect or birefringence. Since the waveguide is designed and fabricated such that there will be no dichroism, (A3) and (A4) only have to be corrected for the influence of birefringence which causes an additional retardation. Since τ_2 describes the phase retardation in absence of birefringence, this correction, τ_i, has to be added to it, as can be seen in (1) and (4).

ACKNOWLEDGMENT

The authors wish to thank F. H. Groen of Delft University of Technology, The Netherlands, for the design of the electrode structure and his support during the research.

REFERENCES

[1] L. G. Kazovski "Multichannel coherent optical communications systems," *J. Lightwave Technol.* , vol. 5, no. 8, pp. 1095–1102, 1987.
[2] T. Okoshi and Kikuchi, *Coherent Optical Fiber Communications*. Dordrecht: KTK Scientific Publishers, 1988.
[3] T. Okoshi, S. Ryu, and K. Kikuchi, "Polarization diversity receiver for heterodyne/ coherent optical fiber communications," in *Proc. 4th IOOC* (Tokyo, Japan), 1983, pp. 386–387.
[4] I. M. I. Habbab and L. J. Cimini, "Polarization-switching techniques for coherent optical communications," *J. Lightwave Technol.*, vol. 6, no. 10, pp. 1537–1548, 1988.
[5] M. W. Meada and D. A. Smith, "New polarization-insensitive direction scheme based on fibre polarisation scrambling", *Electron. Lett.*, vol. 27, no. 1, pp. 10–12, 1991.
[6] J. M. P. Delavaux *et al.*, "All polarization maintaining fibre DPSK transmission experiment," *Electron. Lett.*, vol. 24, no. 21, pp. 1335–1336, 1988.
[7] M. J. Creaner, R. C. Steele, G. R. Walker, and N. G. Walker, "565 Mbit/s optical DPSK transmission system with endless polarization control," *Electron. Lett.*, vol. 24, no. 5, pp. 270–271, 1988.
[8] Y. Okoshi, N. Fuyaya, and Y. Cheng, "New polarization state control device: rotatable fiber cranks", *Electron. Lett.*, vol. 21, no 20, pp. 895–896, 1985.
[9] G. R. Walker and N. G. Walker, "Rugged all fibre endless polarization controller," *Electron. Lett.*, vol. 24, no. 22, pp. 1353–1354, 1988.
[10] S. Thaniyavarn, "Wavelength-independent, optical-damge-immune $LiNbO_3$ TE-TM mode convertor", *Opt. Lett.*, vol. 11, no. 1, pp. 39–41, 1986.
[11] H. Heidrich *et al.*, "Polarization transformer on Ti:$LiNbO_3$ with reset-free optical operation for heterodyne/homodyne receivers," *Electron. Lett.*, vol. 23, no. 7, pp. 335–336, 1987.
[12] N. G. Walker, G. R. Walker, and J. Davidson, "Endless polarization control using an integrated optic lithium niobate device," *Electron. Lett.*, vol. 24, no. 5, pp. 266–268, 1988.
[13] S. Betti, F Curti, B. Daino, G. de Marchis, and E. Iannone, "State of polarization and phase noise independent coherent optical transmission system based on stokes parameter detection," *Electron. Lett.*, vol. 24, no. 23, pp. 1460–1461, 1988.
[14] A. Yariv, *Quantum Electronics*. New York: Wiley, 1967, pp. 296–309.
[15] R. Noé *et al.*, "Comparison of polarization handling methods in coherent optical systems," *J. Lightwave Technol.*, vol. 9, no. 10, pp. 1353–1366, 1991.
[16] N. G. Walker and G. R. Walker, "Polarisation control for coherent optical fibre systems," *Br. Telecom Technol. J.* , vol. 5, no. 2, pp. 63–76, 1987.
[17] P. S. Theocaris and E. E. Gdoutos, *Matrix theory of Photo-elasticity*. Berlin: Springer Verlag, 1979, pp. 56–63.
[18] M. Born and E. Wolf, *Principles of optics*. Oxford: Pergamon Press, 1980, p. 47.
[19] J. J. G. M. van der Tol and J. H. Laarhuis, "A polarization splitter on $LiNbO_3$ using only titanium diffusion," *J. Lightwave Technol.*, vol. 9, no. 7, pp. 879–886, 1991.
[20] A. Rauber, *Current Topics Material Science, no. 1*, E. Kalbis, Ed. Amsterdam: Noord Holand, 1978, pp. 481–601.

Arjan J. P. van Haasteren was born in Leiden, The Netherlands, in 1966. He received the M.Sc. degree in physics from Delft University of Technology, The Netherlands, in 1990. In 1988 he joined the PTT Research Laboratories to perform research for his master thesis. His activities there comprised the analysis, design, fabrication, and modeling of an integrated optical polarization controller on lithium niobate. In 1990 he started a Ph.D. study in the Optics Research Group at Delft University of Technology concerning the development of a real-time, phase stepped, shearing, speckle interferometer.

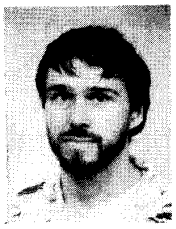

Jos J. G. M. van der Tol was born in Alphen a/d Rijn, The Netherlands, in 1956. He received the M.Sc. and Ph.D. degrees in physics from the State University of Leiden, Leiden, The Netherlands in 1979 and 1985, respectively.

In 1985 he joined the PTT Research Laboratories, where he became involved in research on integrated optical components for use in communication networks. His research interests have covered the modeling of waveguides, the design of electrooptical devices on lithium niobate and their fabrication. At present he is working on guided wave components on III-V semiconductor materials. He is the coauthor of 13 publications in the field of integrated optics.

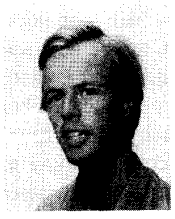

M. Oskar van Deventer was born in Wageningen, The Netherlands, in 1965. From 1983 till 1987 he studied electrical engineering at the University of Technology Eindhoven. He graduated cum laude on monopulse satellite tracking. Since 1987 he has been working at PTT Research on coherent optical communication, polarization effects, frequency management, influence of reflections and bidirectional communication. He is coauthor of more than 12 articles on optical communication.

Hans J. Frankena was born in Haarlem, The Netherlands and received the M.S. and Ph.D. degrees in electrical engineering from the Delft University of Technology. His initial research, as a research assistant at the Department of Electrical Engineering of that especially in waveguides for microwaves. In 1965, he became a lecturer in that department. After his appointment in 1970 as a full professor in Optics at the Department of Applied Physics of the same university, he conducted research in holography, lasers and thin film optics. More recently his attention has also been devoted to integrated optics. From 1971 till 1979 he was the President of the Netherlands' Optics Committee, from 1975 till 1981 a board member of the Netherland's Physical Society, from 1977 till 1979 the President of the European Optical Committee and in the period 1978 till 1987 the Secretary-General of the International Commission for Optics. In 1987, he was elected Fellow of the Optical Society of America and received the President's Award of SPIE.